Photic and non-photic modulation of the mammalian circadian clock

Oosterhout, F.F.T.O. van

ABSTRACT

OBJECTIVE: Mammalian circadian rhythms are driven by the circadian pacemaker of the suprachiasmatic nucleus (SCN) and are synchronized to the external 24-hour light/dark cycle. After advance time zone transitions (eastbound jet lag), overt circadian rhythms require several days to adjust. The retarded adaptation may protect against acute imbalance of different brain systems. Abrupt circadian rhythm changes may trigger migraine attacks, possibly because migraineurs have an inadequate adaptation mechanism. The novel R192Q knock-in migraine mouse model carries mutated $Ca_v2.1$ calcium channels, causing increased presynaptic calcium influx and neurotransmitter release. We investigated whether these mice have an abnormal adjustment to phase advance shifts. METHODS: We examined phase resetting to 6-hour advance shifts of the light/dark cycle with behavioral and electroencephalographic recordings in R192Q and wild-type mice. We recorded excitatory postsynaptic currents in the SCN, and electrical impulse frequency *in vitro* and *in vivo*. RESULTS: R192Q mice showed a more than twofold enhanced adjustment of behavioral wheel-running activity and electroencephalographic patterns, as well as enhanced shifts of electrical activity of SCN neurons *in vivo*. No differences were found for *in vitro* recordings of the electrical impulse frequency in SCN slices. INTERPRETATION: R192Q migraine mice lack the physiological retardation in circadian adaptation to phase advance shifts. The opposite findings *in vivo* and *in vitro* exclude involvement of the retinal input pathway or the phase-shifting capacity of the SCN. Thus, the physiological inhibitory process appears to be mediated by $Ca_v2.1$ channel–dependent afferent signaling from extra-SCN brain areas to the SCN.

INTRODUCTION

Mammalian circadian rhythms in physiology and behavior are driven by a master pacemaker within the suprachiasmatic nucleus (SCN) of the anterior hypothalamus. Individual neurons of the SCN are intrinsically capable of generating a circadian rhythm.[1] To entrain to the environmental light/dark (LD) cycle, light information is conveyed from specialized retinal photoreceptors to the SCN through the retinohypothalamic tract,[2] which utilizes glutamate and pituitary adenylate cyclase-activating peptide as its major neurotransmitters.[3,4] After a shift of the LD cycle, as in time-zone transitions, overt circadian rhythms require several days to regain their phase relation with the new environmental cycle. In humans, this is associated with symptoms of "jet lag." Readjustment to an advanced light schedule (ie, eastbound flights) takes several days more than readjustment to a delayed schedule (ie, flying westbound).[5,6] The reason for this difference and the underlying mechanisms are unknown. Recent evidence suggests that brain pathways outside the SCN attenuate phase advances, but not delays, of the rat circadian system.[7] If the ability to adjust to phase advanced light schedules is dependent on signaling mechanisms within the central nervous system, we expect that animal models with alterations in synaptic signaling show different resetting kinetics.

In this study, we investigate resetting in a migraine mouse model. Migraine is a common brain disorder, characterized by disabling attacks of headache, autonomic dysregulation, and in one third of patients, neurological (aura) symptoms.[8] Attacks can be triggered by acute changes in sleep pattern, such as lack of sleep, sleeping in, and time zone transitions.[8–10] In a family with familial advanced sleep phase syndrome, all carriers of the causative casein kinase I δ clock gene mutation[11,12] also suffered from migraine with aura, suggesting common pathophysiological mechanisms.[13] There is abundant evidence that the migraine brain processes sensory stimuli differently than the brains of nonmigraineurs. Both hyperexcitatory responses to acute and lack of habituation to repeated visual, auditory, or cognitive stimuli have been reported (for review, see Ambrosini and colleagues[14]). Familial hemiplegic migraine type 1 (FHM1) is an autosomal dominant subtype of migraine in which attacks are associated with hemiparesis.[15] The headache and aura symptoms are otherwise identical to those of the common forms of migraine, and the majority of FHM patients also have normal, "nonhemiplegic" migraine attacks.[16,17]

We recently generated knock-in mice expressing the R192Q *CACNA1A* mutation that, in humans, causes FHM1.[18,19] The *CACNA1A* gene encodes the pore-forming α1A

subunit of voltage-gated $Ca_v2.1$ (P/Q-type) calcium channels.[18] These channels are predominantly localized at presynaptic nerve terminals throughout the brain,[19] including the SCN,[20–23] and play a key role in mediating neurotransmitter release.[24,25] R192Q mice show enhanced single-channel calcium influx, associated with increased spontaneous and triggered neurotransmitter release, and enhanced susceptibility for cortical spreading depression.[19,26] Cortical spreading depression is the likely underlying mechanism for migraine aura[27,28] and may trigger migraine headache pathways in animals[29] and possibly humans.[30]

Here, we examined the behavioral and electrophysiological responses of R192Q mice to 6-hour advance shifts to explore the hypothesis that $Ca_v2.1$ calcium channels are involved in the neuronal signaling process from afferent pathways onto the SCN, and thus may play an important role in retarded adjustment to advance phase shifts. Indeed, wheel-running activity rhythms of R192Q mice showed enhanced advancing responses, and recordings of electroencephalographic (EEG) parameters showed an enlarged shifting capacity of the sleep/wake cycle in mutated mice, suggesting atypical phase resetting of their circadian system. Recordings of excitatory postsynaptic currents (EPSCs) in the SCN and of electrical impulse frequency *in vitro* and *in vivo* support the hypothesis that the physiological inhibition of advance phase resetting is mediated via $Ca_v2.1$ channel–dependent afferent signaling from extra-SCN brain areas onto the SCN.

MATERIALS AND METHODS

R192Q Knock-in Mice

We used a knock-in mouse strain carrying the human FHM1 R192Q mutation (i.e., an arginine-to-glutamine change at amino acid 192) in *Cacna1a,* the mouse ortholog of the human *CACNA1A* gene.[19] Male R192Q mice and littermates were genotyped after weaning as described previously.[19] Genotypes were confirmed at the end of each experiment. Adult mice were housed individually in cages equipped with a running wheel in a temperature-controlled room (22°C). Time of lights on is defined as "Zeitgeber time" (ZT) 0, and time of lights off as ZT 12. Food and water were available ad libitum. The presence of wheelrunning activity was automatically recorded in 1-minute bins. All experiments were performed under the approval of the Animal Experiments Ethical Committee of the Leiden University Medical Center.

Wheel-Running Activity Rhythms

After entrainment to a 12/12 LD regimen for 4 weeks, advances or delays of the light cycle were achieved by starting the light time 6 hours earlier or by ending it 6 hours later, respectively.[7,31] In both protocols, animals were exposed to one additional shifted light cycle.[7,31] After exposure to the shifted light cycles, the animals were released into constant darkness (DD) for at least 14 days to determine the phase shift in the absence of possible masking effects of light. The magnitude of the steady-state behavioral phase shift was determined by manually fitting straight lines through the activity onsets before and after the shift of the LD cycle and extrapolating these lines to the first day after the shift. Transient days immediately after the shift were excluded from analysis. In addition, a day-to-day analysis was performed by measurement of activity onsets after the shift in DD relative to the unperturbed old phase predicted by the free-running period. The free-running period was determined for days 5 to 14 in DD using periodogram analysis.

Sleep/Wake Recordings

Techniques for EEG and electromyographic (EMG) recordings were as described previously.[32,33] Male R192Q mice and wild-type control mice (minimum age, 12 weeks; 20–30gm) were entrained to a 12/12-hour LD cycle. The animals were anesthetized by intraperitoneal injection (Ketamine Hydrochloride [Nimatek], 100mg/ml, 75mg/kg; medetomidine hydrochloride [Domitor], 0.5mg/ml, 0.5mg/kg). EEG electrodes were screwed through the skull on the dura over the right cortex and the cerebellum. For EMG recordings, two isolated wires with suture patches were inserted between the skin and the neck muscle tissue. The animals were connected to the recording system by a flexible cable and a swivel system, causing minimal interference with the animals' movements. After an 18-hour baseline recording, starting at lights on, the LD schedule was advanced by 6 hours as described earlier. The recordings were continued after release into DD. The EEG and EMG signals were amplified (approximately 2000X), band-pass filtered (0.5–30Hz, -40 DB/decade), and subjected to analog-to-digital conversion (sampling rate, 128Hz). Three vigilance states (waking, non–rapid eye movement sleep, and REM sleep) were determined visually for every 4-second epoch from standardized EEG/EMG criteria for mice.[32,33] The onset of waking was defined as the onset of the first three 30-minute intervals with waking values above the 24-hour mean. Individual phase shifts were determined by comparing the onset of waking on the second day in DD with the unshifted baseline values. The second day in DD was used because LD cycles may have aftereffects on sleep on day 1 in DD in rats[34,35] and mice.[36]

Light Conditions

Wheel-running activity patterns of R192Q and wild-type mice were examined in the following light protocols: LD 12/12 hours for 3 weeks, constant darkness (DD) for 3 weeks, and constant light (LL) for 3 weeks (approximately 200 lux during lights on). Periodogram analyses with 5-minute resolution were performed over the last 10 days in each light condition. The phase angle of entrainment was determined by extrapolating the phase of the free-running rhythm after release into DD to the last day of the LD cycle.

Response to Brief Light Pulses

Partial-phase response curves to brief light pulses (15 min, 500 lux) were constructed for wild-type and R192Q mice. Because we were mainly interested in the generation of phase advances, we concentrated on the second part of the night and applied pulses at circadian time (CT) 19, 21, 23, 1, or 3 (CT 12 = activity onset) on the seventh day in DD. Steady-state phase shifts of wheel-running rhythms were determined as described earlier.

Whole-Cell Recordings of Excitatory Postsynaptic Currents

Brain slice preparation and patch recording methods were similar to earlier studies.[37,38] Mice were killed by decapitation during the day (ZT 6), and brains dissected and placed in cold oxygenated artificial cerebrospinal fluid containing (in mM) NaCl 130, $NaHCO_3$ 26, KCl 3, $MgCl_2$ 5, NaH_2PO_4 1.25, $CaCl_2$ 1.0, glucose 10 (pH 7.2–7.4). After cutting slices (VT 1000S; Leica, Wetzlar, Germany) from areas of interest, transverse sections (350μm) were placed in artificial cerebrospinal fluid (25–27°C) for at least 1 hour (in this solution, $CaCl_2$ is increased to 2mM, $MgCl_2$ is decreased to 2mM). Slices are constantly oxygenated with 95% O_2-5% CO_2 (pH 7.2–7.4, osmolality 290–310mOsm). Slices were viewed with an upright compound microscope (Axioskop FS2A plus; Zeiss, Göttingen, Germany), using a water immersion lens (40X), differential interference contrast optics, and an infrared-sensitive video camera (Optronis, VX45, Kehl, Germany). This imaging technique allowed us to distinguish between dorsal and ventral SCN regions. For recordings of postsynaptic currents, patch electrodes were pulled on a two-stage puller (P10; Narashige, Tokyo, Japan). Electrode resistance in the bath was typically 3 to 6MΩ. The standard solution in the patch pipette for measurement of spontaneous postsynaptic currents contains (in mM) K-gluconate 112.5, Hepes 10, MgATP 5, NaCl 4, EGTA 1, $MgCl_2$ 1, $CaCl_2$ 0.5, GTP-Tris 1, leupeptin 0.1, and phosphocreatine 10. The pH was adjusted to 7.25 to 7.3 using potassium hydroxide, and the osmolality to 290 to 295mOsm using sucrose. Bicuculline (20μM) was added to the bath solution to

block inhibitory GABAA-mediated synaptic transmission. The glutamate receptor (alpha-amino-3-hydroxy-5-methyl-4-isoxazole propionic acid/kainate) antagonist 6-cyano-7-nitroquinoxaline-2,3-dione (CNQX; 20μM) was added to the bath to test the nature of the remaining excitatory events. Whole-cell recordings were obtained with a commercial patch amplifier (EPC-10; HEKA, Lambrecht, Germany) and monitored on-line with the data acquisition software PATCHMASTER (HEKA). After obtaining a GΩ-seal and obtaining whole-cell configuration, cell capacitance and access resistance were compensated, and recording was then initiated. Series and input resistance were monitored repeatedly by checking the response to small test pulses (10mV) from the holding potential (-80mV). Spontaneous postsynaptic currents were analyzed using the MiniAnalysis program (Synaptosoft, Decatur, GA, USA). The software was used to automatically detect the spontaneous EPSCs (sEPSCs) in 4-minute-long, gap-free recordings. Each event was manually checked to exclude artifacts. The mean frequency of the EPSCs was calculated for each neuron.

In Vitro Electrophysiology Experiments

After a 6-hour advance of the light cycle, multiunit activity rhythms of SCN neurons were recorded as described previously.[39] In brief, coronal hypothalamic slices (500μm) were prepared at the end of the light period of the second shifted light cycle (new ZT 12) for all experiments in both groups of animals. Preparation time in the control (unshifted) animals was also at the end of the light period (ZT 12). This preparation time was chosen to conform to protocols that Yamazaki and colleagues[31] and Vansteensel and coauthors[7] used. The slices were then kept submerged in a laminar flow recording chamber and were continuously perfused with oxygenated artificial cerebrospinal fluid (36°C, 95% O_2, 5% CO_2). Dorsal and ventral regions were mechanically separated by a horizontal cut, which prevents communication between these areas. As a result, the recorded rhythm reflects the endogenous phase of each subregion.[39] Extracellular electrical activity was recorded by two stationary platinum/iridium metal electrodes (75μm, insulated) placed in either subregion of the SCN. The signals were amplified with a low noise amplifier and were band-pass filtered. Action potentials were selected by spike triggers (signal-to-noise ratio > 2:1) and counted electronically every 10 seconds for at least 36 hours for both dorsal and ventral regions separately.

In Vivo Electrophysiology Experiments

Techniques for *in vivo* recording of SCN electrical activity have been previously described for the rat.[7,40] In brief, mice (minimum age, 12 weeks; 20–30gm) were entrained to a 12/12 LD cycle and anesthetized by intraperitoneal injection of a

mixture of Nimatek (100mg/ml, 75mg/kg) and Domitor (0.5mg/ml, 0.5mg/kg). Tripolar stainless steel microelectrodes (Plastics One, Düsseldorf, Germany) were implanted, consisting of two twisted electrodes (polyimide insulated; bare electrode diameter, 0.125mm) for differential recording that were aimed at the SCN, and a third uncoated electrode that was placed in the cortex for a reference. The electrical signal was amplified, bandwidth filtered, and recorded by a data acquisition system. Spike triggers were set to detect multiunit neuronal activity, and action potentials were counted in 10-second bins. After a minimum of four unambiguous peaks in LD, the LD schedule was advanced by 6 hours as described earlier. The recordings were continued for 3 days in DD after the shift. At the end of each experiment, the site of recording was verified by histology.

Analysis of In Vitro and In Vivo Electrophysiology Experiments

Electrical activity rhythms obtained *in vitro* and *in vivo* were smoothed.[41] Peak times were determined off-line and were used as a phase marker to establish the magnitude of the phase shift. Phase shifts of *in vivo* SCN neuronal activity rhythms were determined by comparing peak times on days 1 to 3 in DD with the averaged peak time before the shift. Ambiguous peaks were excluded from analysis. The averaged peak times of *in vitro* and *in vivo* recordings were tested using two-way analyses of variance (ANOVAs). A paired *t* test was used to compare peak times between ventral and dorsal SCN *in vitro*.

RESULTS

Characterization of R192Q Mice

WHEEL-RUNNING RECORDINGS. Behavioral resetting characteristics in wild-type and R192Q mice were determined by analyses of wheel-running activity rhythms after exposure to either a 6-hour advance or delay of the 12/12 LD cycle, followed by DD. After a 6-hour advance of the 12/12 LD cycle, the steady-state wheel-running activity onset was shifted by 1.5 hours (± 0.2) in wild-type mice ($p < 0.001$, n = 8, paired *t* test; **Figs 1A, C**). All R192Q mice responded with significantly larger advances ($p < 0.001$, independent *t* test), averaging 3.6 hours (± 0.3) in steady-state ($p < 0.001$; n = 8; paired *t* test; see **Figs 1A, C**). Day-to-day analysis showed significant phase advances for both genotypes on days 2 to 9 after the shift of the LD cycle ($p < 0.05$, ANOVA with post hoc Dunnett's tests). Comparison of the results between R192Q and wild-type mice demonstrated that R192Q mice showed significantly larger phase advances than the wild-type mice every day after the shift ($p < 0.05$, two-

way ANOVA, significant effect of genotype, with post hoc independent *t* tests; see **Fig 1D**). Free-running periods (τ) in DD were comparable in the two genotypes (wild-type: τ = 23.8 ± 0.1 hour; R192Q: τ = 23.9 ± 0.1 hour; p > 0.1, independent *t* test).

After a 6-hour delay of the LD cycle, both wild-type (n = 8) and R192Q (n = 8) mice displayed an equally large steady-state phase delay of their wheel-running rhythms (*p* > 0.5, independent *t* test): wild-type and R192Q rhythms were shifted by -4.3 (± 0.2) and -4.4 hours (± 0.1), respectively (*p* < 0.001, paired *t* tests; see **Figs 1B, C**). Day-to-day analysis of activity onsets demonstrated significant delays on days 1 to 9 after the shift (*p* < 0.001, ANOVA with post hoc Dunnett's tests), without genotypic differences (*p* > 0.5, two-way ANOVA; see **Fig 1E**).

SLEEP/WAKE RECORDINGS. Analysis of EEG and EMG patterns provided supportive evidence for enhanced resetting of behavioral parameters in R192Q mice. After a 6-hour advance of the 12/12 LD cycle, the onset of waking was phase advanced by 1.1 hours (± 0.4) in wild-type mice (n = 4) and 2.5 hours (± 0.1) in R192Q mice (n = 4; **Fig 2**). The circadian phase of waking onset in the R192Q mice deviated from unshifted control values (*p* < 0.001, paired *t* test), whereas wild-type mice did not shift significantly (*p* > 0.05, paired *t* test). R192Q mice responded with significantly larger advances than the control animals (*p* < 0.05, independent *t* test).

LIGHT CONDITIONS. The circadian phenotype of R192Q mice was examined under different experimental light regimens: 12/12 LD, DD, and LL (see **Supplementary Figs 1A, B**). Under 12/12 LD cycles, R192Q mice showed 87% of total wheel-running activity as compared with wild-type control mice and entrained normally to the light cycle. No phase jump was shown on release in DD (phase angle ψ: wild-type, 0.06 ± 0.03 hour; R192Q, 0.15 ± 0.03 hour). Under DD and LL, no differences were observed in period length between R192Q (n = 8) and wild-type (n = 8) mice (*p* > 0.1, two-way ANOVA; see **Supplementary Figs 1A, B**).

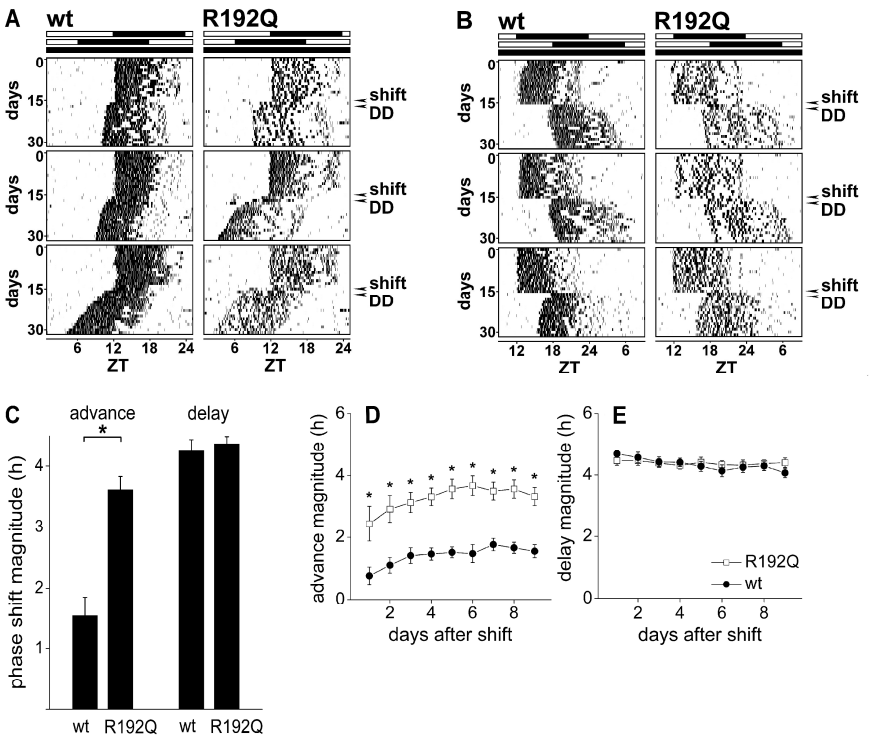

Figure 1. Steady-state and day-to-day phase shifts of wheel running behavior in R192Q and wild-type mice following a 6-h advance or delay of the LD cycle. **(A)** Wheel running rhythms of three wild-type (left) and three R192Q (right) mice, exposed to a 6-h advance of the LD 12:12 cycle (onset shift indicated by the first arrow head). After the advance of the light cycle, the animals were released into constant darkness (onset DD indicated by the second arrow head). Above the records, the LD schedule before, during, and after the shift is indicated (white, lights on; black, lights off). The x-axis represents the Zeitgeber time (ZT) before the shift, the y-axis represents the subsequent days. **(B)** Wheel running rhythms of three wild-type (left) and three R192Q (right) mice, exposed to a 6-h delay of the LD 12:12 cycle (onset shift indicated by the first arrow head). After the delay of the light cycle, the animals were released into constant darkness (onset DD indicated by the second arrow). The figure layout is similar to Fig. 1A. **(C)** Average (± s.e.m.) steady-state phase shift magnitude of wheel running rhythms in wild-type and R192Q mice in response to the 6-h phase advance (left bars) and 6-h delay (right bars) of the LD schedule. The behavioral advances of R192Q mice were significantly larger than those of wild-type mice ($p < 0.001$, independent t-test), while delays did not differ. **(D,E)** Day-to-day analysis of the phase shift magnitude (± s.e.m.) of the activity onset following the 6-h phase advance (D) and delay (E) of the LD cycle in wild-type and R192Q mice. The x-axes show the days in DD after the shift, the y-axes indicate the phase shift magnitude in h. The phase advances of wild-type mice differed significantly from those obtained in R192Q mice at days 1-9 after the shift (asterisks: $p < 0.05$, two-way ANOVA, significant effect of genotype, with post hoc independent t-tests). Following the 6-h delay, the two genotypes showed phase shifts of similar magnitude ($p > 0.5$, two-way ANOVA).

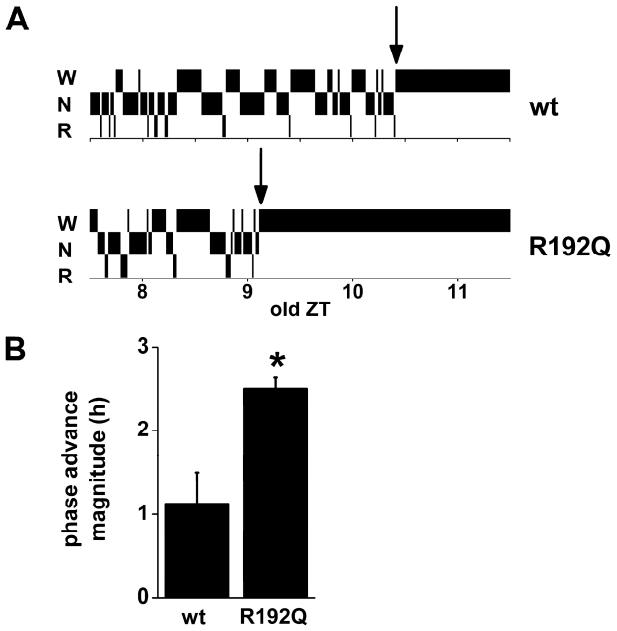

Figure 2. Sleep-wake patterns in wild-type and R192Q mice after exposure to a 6-h advance of the LD cycle. (A) A representative 12-h record of vigilance states (W=waking, N=non-REM sleep, R=REM sleep) obtained during the second day in DD following the 6-h advance of the LD cycle from one wild-type mouse (upper graph) and one R192Q mouse (lower graph). Arrows indicate the onset of waking, which was defined as the onset of the first three 30-min intervals with waking values above the 24h mean. Each data point is the mean of 15 4-s epochs (1 min). The x-axis indicates old ZT (ZT before the shift) in h. **(B)** Average (± s.e.m.) phase shift magnitude of the onset of waking determined after the 6-h advance of the LD cycle (asterisk: $p < 0.05$; independent t-test).

PHASE RESPONSE TO BRIEF LIGHT PULSES. Fifteen-minute saturating light pulses were given at CT 19, 21, 23, 1, and 3 to generate phase advances of the wheel-running activity rhythm (wild-type: n = 5; R192Q: n = 7; see **Supplementary Fig 1C**). Two-way ANOVA showed no significant differences between genotypes ($p > 0.6$), although there was a significant effect of genotype x time ($p < 0.05$), which is caused by a displacement of the phase response curve of about 0.5 to 1 hour along the *x*-axis. No differences in the maximal advancing response ($\Delta\phi_{max}$) of the wheel-running activity rhythms were observed between genotypes (wild-type $\Delta\phi_{max}$ = 0.5 ± 0.1 hour, n = 7; R192Q $\Delta\phi_{max}$ = 0.6 ± 0.1 hour, n = 12; $p > 0.3$, independent *t* test). Independent *t* tests performed on each circadian time point demonstrated no significant differences either ($p > 0.06$).

EXCITATORY POSTSYNAPTIC CURRENT RECORDINGS. To examine whether excitatory synaptic signaling is changed in the SCN of R192Q versus wild-type mice, we measured sEPSCs in SCN slices during the day (**Fig 3**). Whole-cell recordings were obtained from dorsal SCN neurons, which receive excitatory input.37 Bicuculline was added to the bath to suppress inhibitory activity. In R192Q mice, the remaining sEPSCs were blocked by the AMPA/KA glutamate receptor (GluR) antagonist CNQX (20μM; 9/9 neurons), as previously demonstrated in wild-type mice.[37] Nearly a fivefold increase was observed in frequency of sEPSCs in R192Q mice, averaging 0.44 ± 0.11Hz in wild-type (n = 11) and 2.13 ± 0.57Hz in R192Q mice (n = 9).

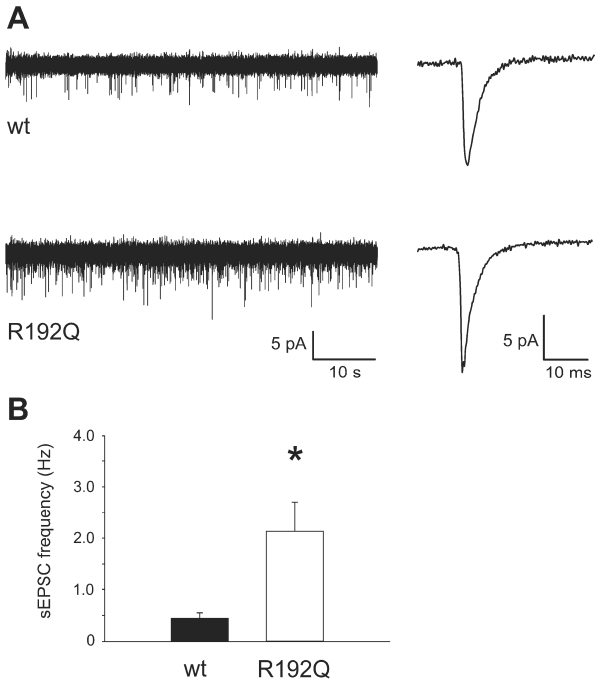

Figure 3. Recordings of spontaneous EPSCs in dorsal SCN neurons. (A) Examples of spontaneous postsynaptic currents recorded in the day in hypothalamic slices from wild-type and R192Q mice. Note the increased frequency in the left panels. The right plots show averaged sEPSCs for wild-type (n = 64) and R192Q (n = 184) mice. **(B)** The mean frequency of sEPSCs in dorsal SCN cells from R192Q mice (n = 9) is significantly enhanced compared to neurons from wild-type mice (n = 11, $p < 0.01$).

In Vitro Electrophysiology

To examine whether phase shifting of wheel-running activity coincided with the phase-shifting response of the SCN itself, we recorded electrical activity rhythms in the SCN *in vitro* (**Fig 4**; see Supplementary **Fig 2**). Brain slices were prepared at the onset of DD. A horizontal cut separated dorsal and ventral regions from which recordings were performed simultaneously. Peaks of electrical activity rhythms in unshifted LD cycles occurred shortly before midday in both genotypes (see Supplementary **Fig 2E**). To determine phase shifts, we compared peak times of recordings from phase-advanced animals (wild-type: dorsal, n = 6; ventral, n = 4; R192Q: dorsal, n = 7; ventral, n = 6) with peak times of the unshifted controls (wild-type: dorsal, n = 7; ventral, n = 7; R192Q: dorsal, n = 5; ventral, n = 4). Considerable advances were found in the electrical activity rhythms of ventral and dorsal SCN of both genotypes ($p < 0.001$, two-way ANOVA with post hoc independent *t* tests; see **Fig 4E**). The ventral SCN was shifted by 5.4 hours (± 0.5) in wild-type and 3.8 hours (± 1.0) in R192Q mice. The dorsal SCN was shifted by 4.7 hours (± 0.9) in wild-type and 3.5 hours (± 1.2) in R192Q mice. Notably, rhythms of R192Q mouse SCN were not shifted to a larger extent than wild-type SCN ($p > 0.2$, two-way ANOVA). No significant differences were found between ventral and dorsal recordings in either genotype ($p > 0.05$; paired *t* tests; for details, see **Supplementary Fig 2E**).

In Vivo Electrophysiology

To assess whether the magnitude of phase advances of the SCN was affected by extra-SCN areas, we successfully recorded electrical activity rhythms of the SCN in vivo in four wild-type and four R192Q mice (**Fig 5**). Average SCN peak times before the shift were ZT 6.3 hours (± 0.6) in wild-type mice and ZT 6.9 hours (± 1.2) in R192Q mice. SCN rhythms of R192Q mice showed substantial advances on days 1 to 3 after the shift of the LD schedule, whereas smaller shifts were observed in wild-type SCN (see **Fig 5B**). This difference in phase-shift magnitude between genotypes was significant ($p < 0.05$, two-way ANOVA, significant effect of genotype, with post-hoc independent *t* tests; see **Fig 5B**).

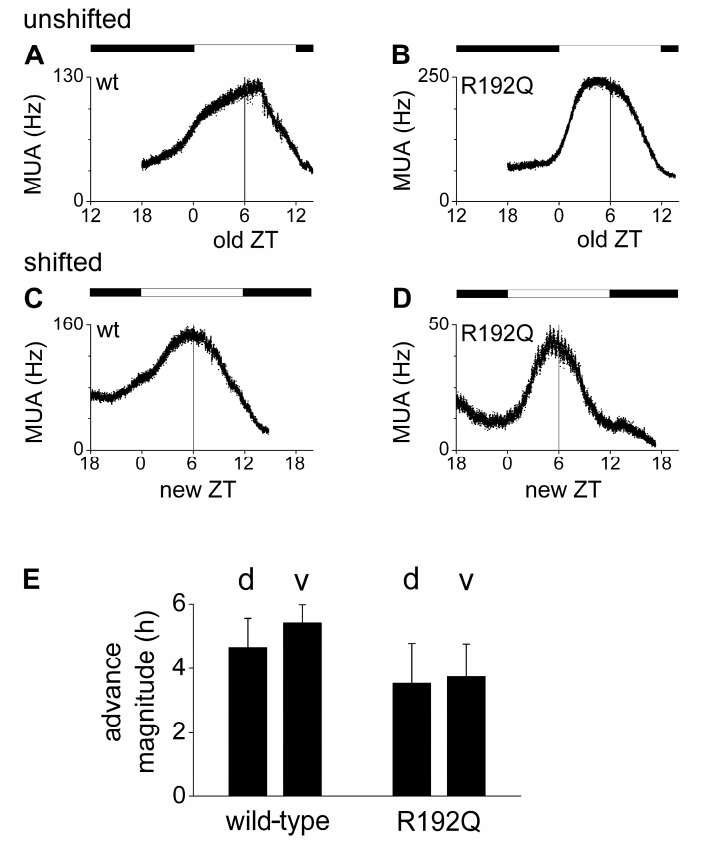

Figure 4. In vitro electrical activity recordings of the SCN in wild-type and R192Q mice after exposure to a 6-h phase advance of the LD cycle. (A,B) Examples of multiunit activity recordings of the dorsal SCN from wild-type (A) and R192Q (B) animals that were not exposed to a shift. For ventral SCN, see Supplementary Fig. 2. **(C,D)** Examples of multiunit activity recordings of the dorsal SCN from wild-type (C) and R192Q (D) animals that were exposed to a 6-h phase advance of the LD cycle. The LD cycle prior to slice preparation is indicated above the records, the shifted LD schedule is represented by the bar in the lower panel (white, lights on; black, lights off). 'Old ZT' (A,B) and 'new ZT' (C,D) is shown on the x-axis and ZT6 is indicated by a vertical line. **(E)** Averaged (± s.e.m.) phase shift magnitudes of in vitro electrical activity rhythms in wild-type and R192Q mice in response to the 6-h phase advance, specified for dorsal (d) and ventral (v) SCN.

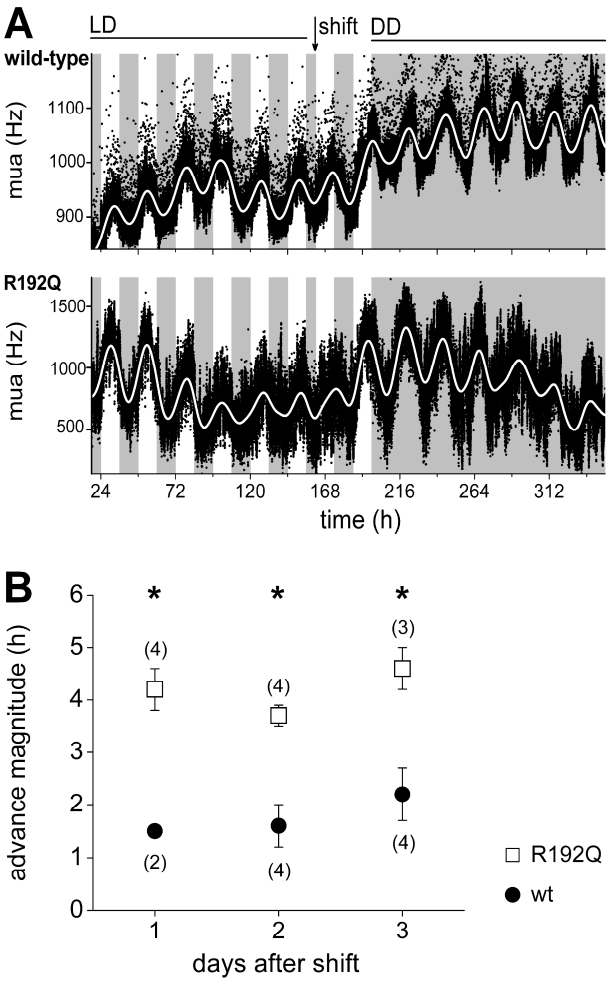

Figure 5. In vivo electrical activity recordings in SCN in wild-type and R192Q mice after exposure to a 6-h phase advance of the LD cycle. (A) Examples of multiunit activity recordings from one wild-type and one R192Q animal that were exposed to a 6-h advance of the LD cycle. The shaded background indicates the times of lights off. The data were smoothed (indicated by the white line) in order to determine peak times. The x-axis indicates time in h, the y-axis shows the multiunit activity. **(B)** Averaged (± s.e.m.) phase shift magnitudes of wild-type and R192Q mice SCN on days 1-3 in DD. Electrical activity rhythms in SCN of R192Q mice showed significantly larger phase shifts as compared to wild-type mice (asterisks: $p < 0.05$, two-way ANOVA, significant effect of genotype, with post hoc independent t-tests). For each day, the number of animals that contributes to the mean is indicated between brackets. The x-axis indicates days in DD after the phase advance of the LD cycle, the y-axis represents the phase shift magnitude.

DISCUSSION

In this study, we examined three main questions: (1) whether wild-type *mice* show retarded adjustment to 6-hour advance, but not to 6-hour delay phase shifts, similar to what has been observed in *rat*; (2) whether the physiological attenuation of circadian adaptation to advance shifting is mediated through $Ca_v2.1$ calcium channels, and whether they exert this action primarily within or outside the SCN; and (3) whether R192Q mutated $Ca_v2.1$ calcium channel mice, as an animal model for migraine, show enhanced phase resetting to 6-hour advance shifts to better understand the triggering mechanism of migraine attacks by circadian rhythm changes.

We first confirmed a similar pattern for phase resetting in wild-type mice as has been previously demonstrated by our group in the rat circadian system[7]: wild-type mice showed a limited capacity to respond to 6-hour advances of the LD cycle (i.e., phase advances of only 1.5 hours), whereas much less inertia was found after 6-hour delays (approximately 4-hour shifts). To address the two other questions, we used R192Q knock-in mice that carry a missense mutation in the α1A subunit of voltage-gated $Ca_v2.1$ calcium channels, which serve a key function in neurotransmitter release[24,25] and may contribute to circadian clock function.[21–23,42–44]

Using wheel-running activity rhythms to characterize behavioral resetting capacity in response to phase shifts, we found identical responses to 6-hour delay shifts in R192Q and wild-type mice (approximately 4 hours). In contrast, in response to 6-hour advance shifts, R192Q mice responded with considerably larger advances compared with wild-type mice (approximately 4 vs 1.5 hours). A difference in the phase advance was already apparent on the first day after the shift and was not associated with significant genotypic differences in free-running rhythms in DD or LL (see **Supplementary Fig 1**). In a small group of animals, we confirmed that the increased advancing response was not specific for wheel-running behavior but was also apparent in the sleep/wake cycle. EEG/EMG recordings showed that sleep/wake patterns were shifted by 2.5 hours in R192Q mice and by 1.1 hours in wild-type mice in the new LD cycle. This is comparable with the observed shifts in wheel-running activity on the same day (i.e., day 2; see **Fig 1D**). These results indicate that an alteration in synaptic signaling through mutant $Ca_v2.1$ channels leads to a lack of the physiological inhibition of phase resetting in response to 6-hour advances of the LD cycle, and consequently to enhanced behavioral phase resetting.

To further characterize the attenuating mechanism responsible for the physiological retardation of adaptation to advance phase shifts, we measured spontaneous AMPA/KA receptor-mediated EPSCs from dorsal SCN neurons in hypothalamic slices. We found an almost fivefold increase in frequency in dorsal SCN neurons of R192Q mice, suggesting that these neurons express modified $Ca_v2.1$ channels and display upregulation of excitatory synaptic transmission. These data are in agreement with the previously reported increased calcium influx through mutated presynaptic $Ca_v2.1$ channels[19,26] and increased neurotransmitter release at the neuromuscular junction of R192Q mice.[19,45]

We also investigated whether the large-magnitude behavioral advances observed in R192Q mice were associated with different phase-shifting capacity of the SCN itself. To this end, we analyzed resetting in an acute slice preparation containing the SCN. Because different regions of the SCN are known to readjust at different rates in response to a shift of the light cycle,[39,46,47] we performed separate electrophysiological recordings from dorsal and ventral SCN regions. Peak times of electrical activity rhythms occurred shortly before the middle of the day in both wild-type and R192Q mice. After the advance of the LD cycle, the electrical activity rhythms from dorsal and ventral SCN *in vitro* were shifted by approximately 4 to 5 hours in both wild-type and R192Q mice. Peaks in the ventral SCN tended to precede the peaks in the dorsal SCN in wild-type animals (see **Supplementary Fig 2E**). These interregional differences were not apparent in R192Q mice. Although we cannot exclude small differences in functional organization within the SCN between the two genotypes, it is notable that the magnitude of the phase shift in the ventral and in the dorsal SCN was substantial in both wild-type and R192Q mice, and cannot explain the difference in behavioral resetting.

The similarity of shifts in wild-type and R192Q mice *in vitro* suggests that the phase-shifting capacity of the SCN itself, including the retinal input pathways, cannot account for the observed behavioral differences. This would agree with the evidence that glutamateinduced phase advances of the SCN predominantly involve L-type (Ca_v1) rather than P/Q-type ($Ca_v2.1$) calcium channels,[48] and with our finding that the phase response curve for 15-minute light pulses was similar in wild-type and R192Q animals (see **Supplementary Fig 1**). We propose, therefore, that the R192Q mutation has affected the interplay between extra-SCN brain areas and the SCN. We tested this hypothesis by recordings of neuronal discharge rhythms in the SCN of freely moving mice in both genotypes. Our results demonstrated that the electrical activity rhythm of the SCN *in vivo*, with functioning brain connections intact, exhibits

significantly larger advancing shifts in R192Q mice than in wild-type animals. The data indicate that signaling pathways between extra-SCN areas and the SCN have a strong capacity to attenuate behavioral phase shifting, rely on $Ca_v2.1$ calcium channels, and have direct impact on the phase of the SCN. Although molecular mechanisms within the SCN have been shown to limit the phase-shifting capacity of the molecular core clock,[46,47,49] this finding identifies an additional level of organization that restricts phase shifting of the circadian system.

We may speculate about a number of putative mechanisms underlying the $Ca_v2.1$-mediated effects on phase resetting. $Ca_v2.1$ channels are common targets of G-protein–linked neuromodulation,[21,50–52] and the R192Q mutation may cause reduced susceptibility to G-protein inhibition of neurotransmitter release.[53] Alternatively, functional coupling to calcium-activated BK potassium channels, which is thought to affect spontaneous firing patterns[54–56] and was implicated in circadian clock function,[43,57,58] may have been altered. This identification of $Ca_v2.1$ channel function in phase resetting opens up the possibility to trace neuroanatomical pathways that retard adjustment to shifted light cycles, particularly when it involves advances.

We used R192Q mice also because they can be regarded as a good model for migraine pathophysiology,[17,19] and changes in sleep pattern and circadian rhythms are known to trigger migraine attacks.[9,10,13] Our findings provide animal experimental evidence that migraineurs may lack the physiological retardation of phase resetting in response to advance shifts, which could theoretically lead to acute imbalance of brain systems leading to attacks. This hypothesis needs to be tested in patients.

Taken together, we provide the first evidence that the physiological inertia in phase resetting is not a property of the pacemaker itself, but rather is mediated by $Ca_v2.1$ channel-dependent afferent signaling from extra-SCN brain areas to the clock. This finding is of potential importance for the development of new strategies to treat jet-lag-related disorders and to further unravel the mechanisms responsible for triggering migraine attacks.

Acknowledgments

This research was supported by Nederlandse Organisatie voor Wetenschappelijk Onderzoek (425-20-403 JHM, Vici 918-56-602 MDF), the EU-funded "Entrainment of the circadian clock"-EUCLOCK (018741 JHM) and EUROHEAD Programs (LSHMCT-2004-504837 MDF), and the Centre for Medical Systems Biology in the framework of the Netherlands Genomics Initiative MDF, AMJMM. We thank H. Duindam and J. Janse for excellent technical assistance, B. Todorov for help with genotyping, and P. Eilers for his suggestions on the statistics. We also thank G. D. Block and W. J. Schwartz for useful comments on the manuscript.

REFERENCES

1. Welsh DK, Logothetis DE, Meister M, Reppert SM. Individual neurons dissociated from rat suprachiasmatic nucleus express independently phased circadian firing rhythms. Neuron 1995;14:697-706.

2. Morin LP, Allen CN. The circadian visual system, 2005. Brain Res Rev 2006;51:1-60.

3. Ebling FJ. The role of glutamate in the photic regulation of the suprachiasmatic nucleus. Prog Neurobiol 1996;50:109-132.

4. Hannibal J, Ding JM, Chen D, et al. Pituitary adenylate cyclase-activating peptide (PACAP) in the retinohypothalamic tract: a potential daytime regulator of the biological clock. J Neurosci 1997;17:2637-44.

5. Aschoff J, Hoffmann K, Pohl H, Wever R. Re-entrainment of circadian rhythms after phase-shifts of the Zeitgeber. Chronobiologia 1975;2:23-78.

6. Revell VL, Eastman CI. How to trick mother nature into letting you fly around or stay up all night. J Biol Rhythms 2005;20:353-365.

7. Vansteensel MJ, Yamazaki S, Albus H, et al. Dissociation between circadian Per1 and neuronal and behavioral rhythms following a shifted environmental cycle. Curr Biol 2003;13:1538-1542.

8. Goadsby PJ, Lipton RB, Ferrari MD. Migraine - current understanding and treatment. N Engl J Med 2002;346:257-270.

9. Fox AW, Davis RL. Migraine chronobiology. Headache 1998;38:436-441.

10. Overeem S, van Vliet JA, Lammers GJ, et al. The hypothalamus in episodic brain disorders. Lancet Neurol1: 2002;437-444.

11. Jones CR, Campbell SS, Zone SE, et al. Familial advanced sleep-phase syndrome: A short-period circadian rhythm variant in humans. Nat Med 1999;5:1062-1065.

12. Xu Y, Padiath QS, Shapiro RE, et al. Functional consequences of a CKIdelta mutation causing familial advanced sleep phase syndrome. Nature 2005;434:640-644.

13. Shapiro RE, Waheed W, Nagle K. A novel familial syndrome of migraine with aura, flushing spells, myalgias, asthma, and the advanced sleep phase syndrome. Cephalalgia 1999;19:424 abstract IV-C1-9

14. Ambrosini A, de Noordhout AM, Sándor PS, Schoenen J. Electrophysiological studies in migraine: a comprehensive review of their interest and limitations. Cephalalgia 2003;23 Suppl 1:13-31.

15. Headache classification subcommittee of the international headache society: The international classification of headache disorders: 2nd edition. Cephalalgia 2004;24:1-160

16. Thomsen LL, Eriksen MK, Roemer SF, et al. A population-based study of familial hemiplegic migraine suggests revised diagnostic criteria. Brain 2002;125:1379-1391.

17. Ferrari MD, van den Maagdenberg AM, Frants RR, Goadsby PJ (2007) Migraine as a Cerebral Ionopathy with Impaired Central Sensory Processing. In Waxman SG ed. Molecular Neurology. New York, USA: Elsevier:439-461.

18. Ophoff RA, Terwindt GM, Vergouwe MN, et al. Familial hemiplegic migraine and episodic ataxia type-2 are caused by mutations in the Ca^{2+} channel gene CACNL1A4. Cell 1996;87:543-552.

19. van den Maagdenberg AM, Pietrobon D, Pizzorusso T, et al. A Cacna1a knockin migraine mouse model with increased susceptibility to cortical spreading depression. Neuron 2004;41:701-710.

20. Westenbroek RE, Sakurai T, Elliott EM, et al. Immunochemical identification and subcellular distribution of the alpha 1A subunits of brain calcium channels. J Neurosci 1995;15:6403-6418.

21. Chen G, van den Pol AN. Presynaptic GABAB autoreceptor modulation of P/Q-type calcium channels and GABA release in rat suprachiasmatic nucleus neurons. J Neurosci 1998;18:1913-1922.

22. Cloues RK, Sather WA. Afterhyperpolarization regulates firing rate in neurons of the suprachiasmatic nucleus. J Neurosci 2003;23:1593-1604.

23. Nahm SS, Farnell YZ, Griffith W, Earnest DJ. Circadian regulation and function of voltage-dependent calcium channels in the suprachiasmatic nucleus. J Neurosci 2005;25:9304-9308.

24. Mintz IM, Sabatini BL, Regehr WG. Calcium control of transmitter release at a cerebellar synapse. Neuron 1995;15:675-688.

25. Wu LG, Westenbroek RE, Borst JG, et al. Calcium channel types with distinct presynaptic localization couple differentially to transmitter release in single calyx-type synapses. J Neurosci 1999;19:726-736.

26. Tottene A, Fellin T, Pagnutti S, et al. Familial hemiplegic migraine mutations increase Ca(2+) influx through single human CaV2.1 channels and decrease maximal CaV2.1 current density in neurons. Proc Natl Acad Sci U S A 2002;99:13284-13289.

27. Lauritzen M. Pathophysiology of the migraine aura. The spreading depression theory. Brain 1994;117:199-210.

28. Hadjikhani N, Sanchez Del Rio M, Wu O, et al. Mechanisms of migraine aura revealed by functional MRI in human visual cortex. Proc Natl Acad Sci U S A 2001;98:4687-4692.

29. Bolay H, Reuter U, Dunn AK, et al. Intrinsic brain activity triggers trigeminal meningeal afferents in a migraine model. Nat Med 2002;8:136-142.

30. Ayata C, Jin H, Kudo C, et al. Suppression of cortical spreading depression in migraine prophylaxis. Ann Neurol 2006;59:652-661.

31. Yamazaki S, Numano R, Abe M, et al. Resetting central and peripheral circadian oscillators in transgenic rats. Science 2000;288:682-685.

32. Huber R, Deboer T, Tobler I. Effects of sleep deprivation on sleep and sleep EEG in three mouse strains: empirical data and simulations. Brain Res 2000;857:8-19.

33. Deboer T, Fontana A, Tobler I. Tumor necrosis factor (TNF) ligand and TNF receptor deficiency affects sleep and the sleep EEG. J Neurophysiol 2002;88:839-846.

34. Borbely AA. Effects of light on sleep and activity rhythms. Prog Neurobiol 1978;10:1-31.

35. Alfoldi P, Franken P, Tobler I, Borbely AA. Short light-dark cycles influence sleep stages and EEG power spectra in the rat. Behav Brain Res 1991;43:125-131.

36. Deboer T, Ruijgrok G, Meijer JH. Short light-dark cycles affect sleep in mice. Eur J Neurosci 2007;26:3518-3523.

37. Michel S, Itri J, Colwell CS. Excitatory mechanisms in the suprachiasmatic nucleus: the role of AMPA/KA glutamate receptors. J Neurophysiol 2002;88:817-828.

38. Michel S, Itri J, Han JH, et al. Regulation of glutamatergic signalling by PACAP in the mammalian suprachiasmatic nucleus. BMC Neurosci 2006;7:15.

39. Albus H, Vansteensel MJ, Michel S, et al. A GABAergic mechanism is necessary for coupling dissociable ventral and dorsal regional oscillators within the circadian clock. Curr Biol 2005;15:886-893.

40. Meijer JH, Watanabe K, Schaap J, et al. Light responsiveness of the suprachiasmatic nucleus: long-term multiunit and single-unit recordings in freely moving rats. J Neurosci 1998;18:9078-9087.

41. Schaap J, Albus H, VanderLeest HT, et al. Heterogeneity of rhythmic suprachiasmatic nucleus neurons: Implications for circadian waveform and photoperiodic encoding. Proc Natl Acad Sci U S A 2003;100:15994-15999.

42. Gompf HS, Moldavan MG, Irwin RP, Allen CN. Nociceptin/orphanin FQ (N/OFQ) inhibits excitatory and inhibitory synaptic signaling in the suprachiasmatic nucleus (SCN). Neurosci 2005;132:955-965.

43. Lundkvist GB, Kwak Y, Davis EK, et al. A calcium flux is required for circadian rhythm generation in mammalian pacemaker neurons. J Neurosci 2005;25:7682-7686.

44. Moldavan MG, Irwin RP, Allen CN. Presynaptic GABA(B) receptors regulate retinohypothalamic tract synaptic transmission by inhibiting voltage-gated Ca^{2+} channels. J Neurophysiol 2006;95:3727-3741.

45. Kaja S, van de Ven RC, Broos LA, et al. Gene dosage-dependent transmitter release changes at neuromuscular synapses of CACNA1A R192Q knockin mice are non-progressive and do not lead to morphological changes or muscle weakness. Neurosci 2005;135:81-95.

46. Nagano M, Adachi A, Nakahama K, et al. An abrupt shift in the day/night cycle causes desynchrony in the mammalian circadian center. J Neurosci 2003;23:6141-6151.

47. Nakamura W, Yamazaki S, Takasu NN, et al. Differential response of Period 1 expression within the suprachiasmatic nucleus. J Neurosci 2005;25:5481-5487.

48. Kim DY, Choi HJ, Kim JS, et al. Voltage-gated calcium channels play crucial roles in the glutamate-induced phase shifts of the rat suprachiasmatic circadian clock. Eur J Neurosci 2005;21:1215-1222.

49. Reddy AB, Field MD, Maywood ES, Hastings MH. Differential resynchronisation of circadian clock gene expression within the suprachiasmatic nuclei of mice subjected to experimental jet lag. J Neurosci 2002;22:7326-7330.

50. Bayliss DA, Li YW, Talley EM. Effects of serotonin on caudal raphe neurons: inhibition of N- and P/Q-type calcium channels and the afterhyperpolarization. J Neurophysiol 1997;77:1362-1374.

51. Silva AP, Carvalho AP, Carvalho CM, Malva, JO. Functional interaction between neuropeptide Y receptors and modulation of calcium channels in the rat hippocampus. Neuropharmacology 2003;44:282-292.

52. Tedford HW, Zamponi GW. Direct G-protein modulation of Cav2 calcium channels. Pharmacol Rev 2006;58:837-62.

53. Melliti K, Grabner M, Seabrook GR. The familial hemiplegic migraine mutation R192Q reduces G-protein-mediated inhibition of P/Q-type (Ca(V)2.1) calcium channels expressed in human embryonic kidney cells. J Physiol 2003;546:337-347.

54. Womack MD, Chevez C, Khodakhah K. Calcium-activated potassium channels are selectively coupled to P/Q-type calcium channels in cerebellar Purkinje neurons. J Neurosci 2004;4:8818-8822.

55. Goldberg JA, Wilson CJ. Control of spontaneous firing patterns by the selective coupling of calcium currents to calcium-activated potassium currents in striatal cholinergic interneurons. J Neurosci 2005;25:10230-10238.

56. Berkefeld H, Sailer CA, Bildl W, et al. BKCa-Ca_v channel complexes mediate rapid and localized Ca^{2+}-activated K^+ signaling. Science 2006;314:615-620.

57. Meredith AL, Wiler SW, Miller BH, et al. BK calcium-activated potassium channels regulate circadian behavioral rhythms and pacemaker output. Nat Neurosci 2006;9:1041-1049.

58. Pitts GR, Ohta H, McMahon DG. Daily rhythmicity of large-conductance Ca^{2+}-activated K^+ currents in suprachiasmatic nucleus neurons. Brain Res 2006;107:54-62.

SUPPLEMENTARY MATERIAL

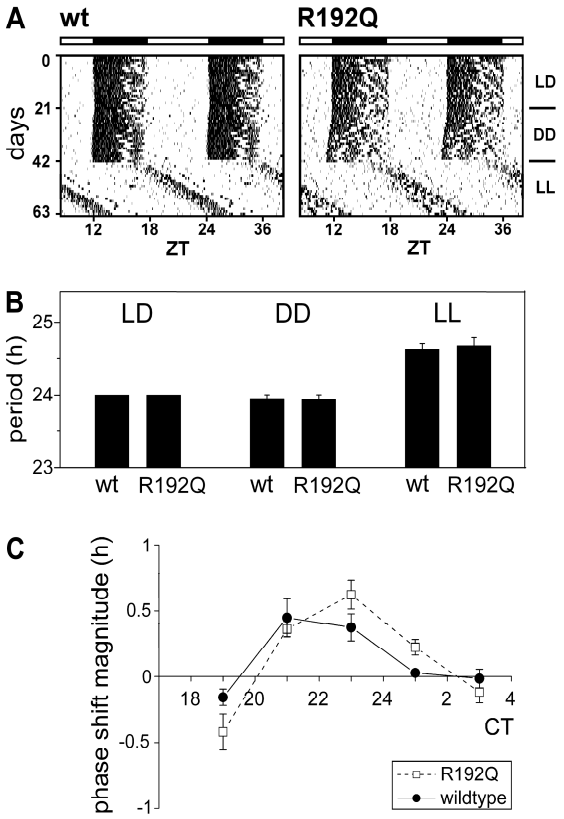

Supplementary Figure 1. Characterization of behavioral circadian phenotype. **(A)** Animals were exposed to LD 12:12 (3 weeks), followed by DD (3 weeks) and LL (3 weeks). Representative double plotted actograms of wild-type (left) and R192Q (right) mice are shown. The initial LD cycle is indicated above the records (white, lights on; black, lights off). The transition to a new light condition is indicated by horizontal lines on the right of the graph. The x-axis indicates ZT, the y-axis represents the subsequent days. All animals entrained to the LD cycle and no phase jump was observed upon release in DD. **(B)** Average (± s.e.m.) period length in each light condition for wild-type and R192Q mice. Free-running period lengths in DD and LL conditions did not differ significantly between wild-type and R192Q mice. Period length was significantly longer in LL as compared to LD and DD in both genotypes (wild-type: τ_{LD} 24.0 ± 0.0, τ_{DD} 24.0 ± 0.1 τ_{LL} 24.6 ± 0.1; R192Q: τ_{LD} 24.0 ± 0.0, τ_{DD} 23.9 ± 0.1, τ_{LL} 24.7 ± 0.1; wild-type $p < 0.05$, R192Q $p < 0.01$; ANOVA with post hoc independent t-test). **(C)** The advance part of the phase response curve, constructed from averaged magnitudes of steady-state phase shifts following 15-min light pulses that were targeted at CT 19 (wild-type -9 ± 4 min, n = 8; R192Q -25 ± 8 min, n = 10), CT 21 (wild-type 27 ± 9 min, n = 7; R192Q 22 ± 4 min, n = 12), CT 23 (wild-type 22 ± 6 min, n = 9; R192Q 37 ± 7 min, n = 12), CT 1 (wild-type 2 ± 2 min, n = 5; R192Q 13 ± 4 min, n = 7) and CT 3 (wild-type -1 ± 4 min, n = 7; R192Q -7 ± 5 min, n = 7). The x-axis indicates the circadian time at the start of the light pulse. The y-axis represents the phase shift produced by the light pulse. A small displacement of the phase response curve along the x-axis is observed for R192Q animals. On the basis of this response curve to brief light pulses, one would have predicted the opposite effect for the responsiveness of R192Q mice on jet-lag phase advances than is observed in the present paper.

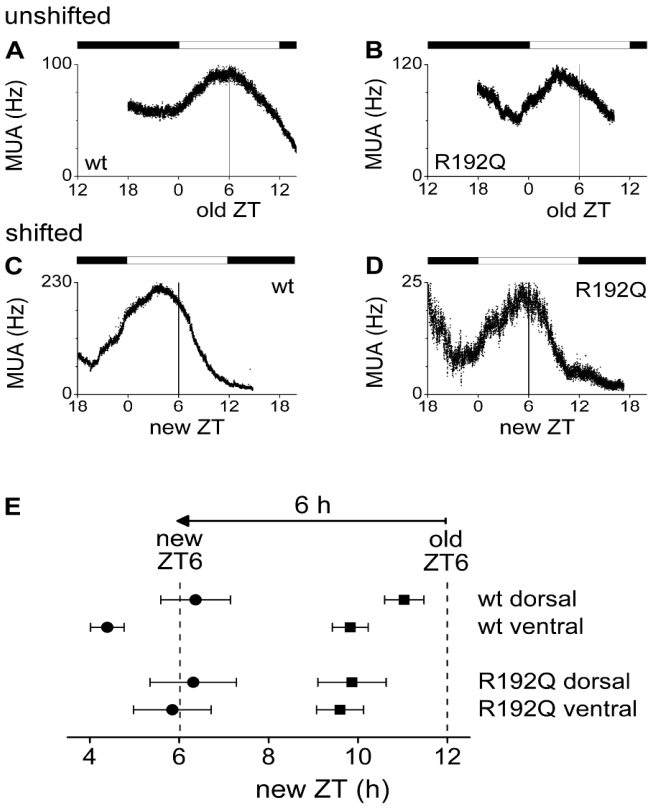

Supplementary Figure 2. In vitro electrical activity recordings of the SCN of wild-type and R192Q mice after exposure to a 6-h phase advance of the LD cycle. Brain slices containing the SCN were prepared at the end of the light period in control and in shifted animals. Dorsal and ventral sections of the SCN were separated by a horizontal cut and electrical activity was recorded simultaneously in the two areas by stationary electrodes. **(A,B)** Examples of multiunit activity recordings of the ventral SCN from wild-type (A) and R192Q (B) animals that were not exposed to a shift. **(C,D)** Examples of multiunit activity recordings of the ventral SCN from wild-type (C) and R192Q (D) animals that were exposed to a 6-h phase advance of the LD cycle. The figure layout is similar to Fig. 4A-D. **(E)** Averaged peak times (± s.e.m.) of multiunit activity rhythms in SCN slices in wild-type (upper part) versus R192Q (lower part) mice. Recordings from the dorsal and ventral parts were analyzed separately and averages are shown per region. After the advance, peak times of ventral and dorsal SCN rhythms were significantly shifted in both genotypes (■ unshifted animals; □ shifted animals). In wild-type mice, the ventral SCN rhythm preceded the dorsal in 6 out of 7 slices under unshifted conditions (averaged 1.2 ± 0.6 h, $p = 0.08$, paired t-test) and in 4 out of 4 slice recordings after the 6-h advance (averaged 2.9 ± 0.5 h, $p = 0.01$, paired t-test). These differences were not statistically significant. No differences were observed between dorsal and ventral recordings in R192Q mice ($p > 0.5$, paired t-tests). Despite enhanced behavioral responses of R192Q mice to a 6-h advance of the LD cycle, the SCN in R192Q mice was not shifted to a larger extent than wild-type mice. The x-axis indicates ZT (h) of the shifted LD cycle. Dashed vertical lines represent unshifted (right) and phase advanced (left) ZT6.